Molecular Microbiology (1999) **34**(5), 1133–1145

A molecular switch in SecA protein couples ATP hydrolysis to protein translocation

Spyridoula Karamanou,[1] Eleftheria Vrontou,[1] George Sianidis,[1] Catherine Baud,[1] Tilmann Roos,[2] Andreas Kuhn,[2] Anastasia S. Politou[3] and Anastassios Economou[1,4]*

[1]Institute of Molecular Biology and Biotechnology and Department of Biology, University of Crete, PO Box 1527, GR-711 10 Iraklio, Crete, Greece.

[2]Department of Molecular Biology and Microbiology, Universitaet Hohenheim-Stuttgart, Germany.

[3]Department of Chemistry, University of Crete, Crete, Greece.

[4]MINOTECH biotechnology, PO Box 1527, GR-711 10 Iraklio, Crete, Greece.

Summary

SecA, the dimeric ATPase subunit of bacterial protein translocase, catalyses translocation during ATP-driven membrane cycling at SecYEG. We now show that the SecA protomer comprises two structural modules: the ATPase N-domain, containing the nucleotide binding sites NBD1 and NBD2, and the regulatory C-domain. The C-domain binds to the N-domain in each protomer and to the C-domain of another protomer to form SecA dimers. NBD1 is sufficient for single rounds of SecA ATP hydrolysis. Multiple ATP turnovers at NBD1 require both the NBD2 site acting *in cis* and a conserved C-domain sequence operating *in trans*. This intramolecular regulator of ATP hydrolysis (IRA) mediates N-/C-domain binding and acts as a molecular switch: it suppresses ATP hydrolysis in cytoplasmic SecA while it releases hydrolysis in SecY-bound SecA during translocation. We propose that the IRA switch couples ATP binding and hydrolysis to SecA membrane insertion/deinsertion and substrate translocation by controlling nucleotide-regulated relative motions between the N-domain and the C-domain. The IRA switch is a novel essential component of the protein translocation catalytic pathway.

Received 8 September, 1999; revised 24 September, 1999; accepted 28 September, 1999. *For correspondence at IMBB, PO Box 1527, GR-711 10 Iraklio, Crete, Greece. E-mail aeconomo@imbb.forth.gr; Tel. (+30) 81 391166; Fax (+30) 81 391166.

Introduction

Polypeptide translocation across the bacterial plasma membrane is catalysed by a complex membrane transporter termed preprotein translocase or translocon (for recent reviews, see Duong *et al*., 1997; Danese and Silhavy, 1998; Economou, 1998, 1999). Translocase is a complex of the membrane proteins SecYEGDFYajC with the peripheral ATPase SecA (Duong *et al*., 1997; Economou, 1998). Only SecYE and SecA comprise the essential enzyme core. Secretory proteins are delivered to the membrane by chaperones and bind to translocase at SecA (Hartl *et al*., 1990; Miller *et al*., 1998). This association triggers multiple turnovers of ATP (Schiebel *et al*., 1991) and leads to SecA cycling, i.e. the transition of SecA between a 'membrane-inserted' and a 'deinserted' state (Economou and Wickner, 1994). SecA membrane cycling may be facilitated by SecG, SecD and SecF (Kim *et al*., 1994; Economou *et al*., 1995; Nishiyama *et al*., 1996; Duong and Wickner, 1997a,b; Matsumoto *et al*., 1997). During cycling, SecA was proposed to operate as a motor-like component (Economou and Wickner, 1994), allowing processive translocase movement along the polymeric substrate (Economou, 1998), in steps of 20–30 aminoacyl residues (Schiebel *et al*., 1991; Uchida *et al*., 1995; van der Wolk *et al*., 1997). Substrates are thought to be transported through a 'pore'-like structure composed of SecYEA (Joly and Wickner, 1993; Meyer *et al*., 1999). SecA cycling is driven by ATP binding and hydrolysis at NBD1, a high-affinity nucleotide binding site (Economou *et al*., 1995; Fig. 1A). The role of NBD2, an essential but non-canonical low-affinity site not known to hydrolyse ATP, remains unknown. The proton motive force enhances SecA deinsertion (Nishiyama *et al*., 1999) and protein translocation (Schiebel *et al*., 1991). Upon complete transfer to the *trans* side of the membrane, the substrate is released. One current hypothesis to explain translocase function is that during the membrane insertion stroke SecA may 'pull-along' the substrate (Economou and Wickner, 1994). However, the precise mechanism by which ATP-derived energy is coupled to substrate forward movement is still a matter of conjecture.

The large SecA dimeric molecule interacts with a bevy of ligands: preproteins (Lill *et al*., 1990; Kimura *et al*., 1991), SecB (Fekkes *et al*., 1997, 1998), nucleotides (Shinkai *et al*., 1991; Mitchel and Oliver, 1993), lipids (Breukink *et al*., 1992, 1995; Ulbrandt *et al*., 1992), SecY

(Ramamurthy and Oliver, 1997) and RNA (Park *et al.*, 1997). We hypothesized that it should be possible to investigate SecA/ligand subreactions by genetic dissection of functional domains. This approach was supported by our finding that SecA can be trypsinized into an N-terminal fragment of 67 kDa, comprising the NBDs and the C-terminal membrane-inserting 30 kDa fragment (Economou and Wickner, 1994; Price *et al.*, 1996).

We now demonstrate that the 67 kDa and the 30 kDa fragments represent distinct structural and functional SecA domains (referred to hereafter as the N-domain and C-domain; Fig. 1A). The N-domain is a constitutive ATPase. Multiple ATP turnovers at NBD1 are regulated *in cis* by NBD2. The two domains physically interact. This association provides an additional level of regulation of ATP hydrolysis *in trans* by the C-domain. A conserved C-domain sequence termed IRA (intramolecular regulator of ATP hydrolysis) operates like a molecular switch: it represses non-productive ATP hydrolysis in cytoplasmic SecA and permits productive, SecY- and substrate-dependent ATP hydrolysis during translocation. These nucleotide interactions stabilize two different SecA conformational states and couple them to substrate translocation in translocase-assembled SecA. Interdomain communication of SecA ATPase through the IRA switch is a novel and essential element of the catalytic pathway of protein translocation.

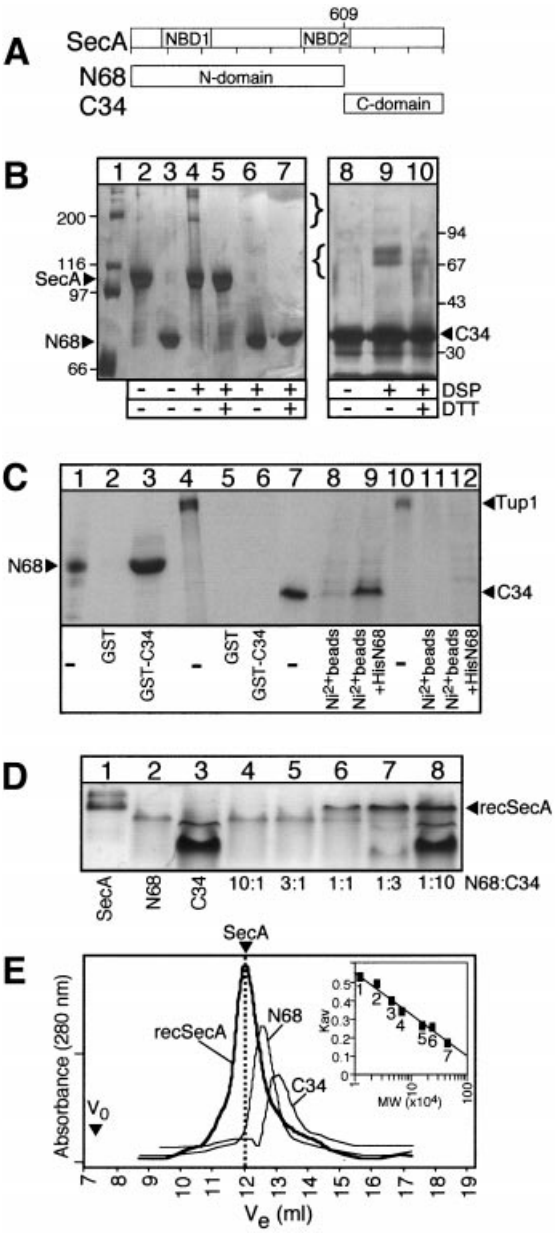

Fig. 1. Physical association of SecA primary domains.
A. Map of SecA and its domains.
B. Chemical cross-linking of SecA, N68 and C34. DSP (20 μM) was added to 2 μM SecA (lanes 4 and 5), 3 μM N68 (lanes 6 and 7) and 5 μM C34 (lanes 9 and 10), in 50 mM Hepes, pH 7.6, 50 mM KCl, 5 mM $MgCl_2$ and 2 mM DTT. Reactions were stopped after 20 min at 0°C by 125 mM Tris-HCl, pH 7.6. Cross-linked, DTT-cleaved (80 mM; 30 min, 37°C) complexes are indicated. Lane 1, MW standards (sizes in kDa); lane 2, SecA; lane 3, N68; lane 8, C34. Samples were subjected to SDS–PAGE (8.5% polyacrylamide for SecA and N68; 15% for C34) followed by silver staining.
C. Physical interaction between SecA domains. One hundred microlitres of suspension of glutathione sepharose with bound GST (lanes 2 and 5), GST-C34 (lanes 3 and 6) and Ni^{2+}-NTA agarose alone (lanes 8 and 11), or with bound His-N68 (lanes 9 and 12), were supplemented with [^{35}S]-N68, [^{35}S]-C34 or [^{35}S]-TUP1 (15 μl; ≈ 50 000 c.p.m.) and incubated (buffer S, 2 h, 4°C). Bound polypeptides were eluted in SDS–PAGE sample buffer, analysed by SDS–PAGE (10% polyacrylamide for lanes 1–6; 15% for lanes 7–12) and fluorography. Lanes 1, 4, 7 and 10 contain 20% of radiolabelled protein.
D. Reconstitution of SecA dimers from purified domains by NATIVE–PAGE: N68 (4 μg), supplemented with C34 at the indicated molar ratios (lanes 4–8), was incubated for 30 min, on ice, in 20 μl buffer B (50 mM Tris, pH 8, 50 mM KCl, 5 mM $MgCl_2$, 2 mM DTT). Lane 1, SecA; lane 2, N68; lane 3, C34. Samples were analysed by NATIVE–PAGE (10%), followed by Coomassie staining. Individual polypeptides and reconstituted complexes (recSecA) are indicated.
E. Reconstitution of SecA dimers from purified domains by gel filtration: N68 (120 μg) or C34 (60 μg) or N68 plus C34, preincubated for 30 min on ice in 50 mM Tris, pH 8/300 mM NaCl/5 mM β-mercaptoethanol, were chromatographed in three separate runs on the same gel filtration column and the three traces were superimposed on the same graph. recSecA, reconstituted SecA; V_0, void volume; inset, MW calibration curve. Protein standards (MW in kDa): inset 1, cytochrome c (12.5); inset 2, chymotrypsin (25); inset 3, albumin (45); inset 4, albumin (68); inset 5, aldolase (158); inset 6, catalase (240), inset 7, ferritin (450).

Results

Synthesis of SecA domains as independent polypeptides

The trypsin-sensitive region around residue 609 (Price *et al.*, 1996) is poorly conserved and contains residues

common to linker sequences (Argos, 1990). This observation, together with the trypsinolysis data (Price *et al*., 1996), suggested that a solvent-exposed linker might connect two independent structural elements. For biochemical characterization, we cloned sequences encoding residues 1–609 and 607–901 as separate genes with or without N-terminal hexahistidinyl extensions (Fig. 1A). The corresponding polypeptides N68 and C34 (MW of 68 and 34 kDa respectively) are soluble and stable *in vivo* and were purified to homogeneity (see *Experimental procedures*). The recombinant polypeptides possess secondary structure [determined by CD (circular dichroism) spectroscopy; data not shown]. Cross-linking using dithiobis (succinimidyl propionate) (DSP) suggested that N68 is monomeric and C34 dimeric (Fig. 1B). Although DTT-sensitive oligomeric SecA ($\geq$ 200 kDa; lanes 4 and 5) and dimeric C34 (70–75 kDa; lanes 9 and 10) were detected, no higher order derivatives of N68 were observed (lane 6). These calculations were corroborated by size-exclusion chromatography: N68 native MW $\approx$ 80–90 kDa and C34 MW$\approx$ 62–68 kDa (Fig. 1E).

These results indicate that each SecA protomer is composed of two structurally independent domains and that the C-domain mediates dimerization.

Physical reconstitution of dimeric SecA from isolated domains

How are the N-/C-domains organized within the SecA protomer? Previous data suggested that the two domains might be in spatial proximity (Shilton *et al*., 1998). This was tested using immobilized N68 and C34 (Fig. 1C). C34 fused C-terminally to glutathione-S-transferase (GST) and was immobilized on glutathione-sepharose (lanes 3 and 6), whereas His-N68 was immobilized on nickel agarose (lanes 9 and 12). [^{35}S]-N68 and [^{35}S]-C34 were incubated with immobilized C34 and N68 respectively. Stable complexes formed on the resins were disrupted by the addition of SDS. [^{35}S]-N68 binds to GST-C34 (more than 60%; lane 3), but not to GST alone (lane 2). Similarly, [^{35}S]-C34 binds to His-N68 (more than 25%; lane 9), but only $\approx$ 4% associates with resin alone (lane 8). [^{35}S]-Tup1, an unrelated yeast protein (Tzamarias and Struhl, 1994), does not bind either GST-C34 or His-N68 (lanes 6 and 12), demonstrating that the SecA primary domains bind to each other with high specificity.

The possibility that the two domains associate has fundamental mechanistic repercussions. To study N-/C-domain complex formation, reactions containing N68 together with increasing amounts of C34 were analysed by native PAGE (Fig. 1D). SecA, N68 and C34 migrate as distinct species (lanes 1–3). Strikingly, in reactions containing both N68 and C34 (above a 1:1 ratio), amounts of N68 were reduced, whereas a novel species migrating at the position of dimeric SecA appeared (lanes 6–8). Immunostaining showed this species to contain both N68 and C34 (data not shown). N68/C34 mixtures (1:1 molar ratio) were also analysed by size exclusion chromatography. A novel species, with an additive absorbance peak and a MW of $\approx$ 180–200 kDa, chromatographs earlier, whereas the individual C34 and N68 peaks disappear (Fig. 1E).

Our data suggest that each SecA protomer is assembled through N-/C-domain association. Formation of dimeric complexes is consistent with stoichiometric N68/C34 association. C-domains from two protomers build the dimer.

Nucleotides alter interdomain interactions in soluble SecA

What is the functional significance of SecA interdomain association? To address this question, we studied N-/C-domain association in the presence of nucleotides known to affect SecA conformation in solution (Shinkai *et al*., 1991; den Blaauwen *et al*., 1996). Limited trypsinolysis of SecA (Price *et al*., 1996) produces 67 kDa, 46 kDa, 34 kDa, 30 kDa and 16 kDa fragments (Fig. 2A, lane 1, and B). Addition of ATP (Fig. 2A, lane 2), ADP (lane 3), or the poorly hydrolysable ATP analogue ATP-γ-S (lane 5) before trypsinolysis causes disappearance of the 46 kDa fragment. Concomitantly, the amounts of the 67 kDa and 34/30 kDa polypeptides increase. The proteolytic profile generated by the non-hydrolysable analogues AMP-PNP (lane 4) and AMP-PCP (lane 6) is identical to that of the apoprotein (lane 1). The 67 kDa fragment is remarkably more stable in the presence of ADP than in its absence, as revealed by trypsinolysis kinetics (Fig. 2C, compare lanes 7, 8–14, 15). Cleavage at 608 is an early event and is not affected by nucleotide (compare lane 2–9). The 46 kDa and the 16 kDa fragments derive from the 67 kDa after cleavage at Arg-419 (Fig. 2B). The 46 kDa accumulates late (lanes 2–7), suggesting that cleavage occurs after separation of the two domains.

Is the C-domain required for N-domain ADP-mediated stabilization? N68 is significantly more susceptible to trypsinolysis in the absence of the C-domain (compare lanes 2–5 in Fig. 2C and E) and is rapidly converted to the 46 kDa (Fig. 2E, lanes 2–5) and 16 kDa fragments (not shown), suggesting that the loop containing residue 419 is facing the N-/C-domain interface. Addition of ATP (Fig. 2D, lane 3), ADP (Fig. 2D, lane 4, and Fig. 2E, lanes 2–9) or ATP-γ-S (lane 6), but not of AMP-PNP or AMP-PCP (lanes 5 and 7), causes reduction of the 46 kDa fragment and concomitantly a remarkable increase in the amount of the 67 kDa fragment.

Our data suggest that SecA exists in an ATP and an ADP state. The ATP state is short-lived because ATP

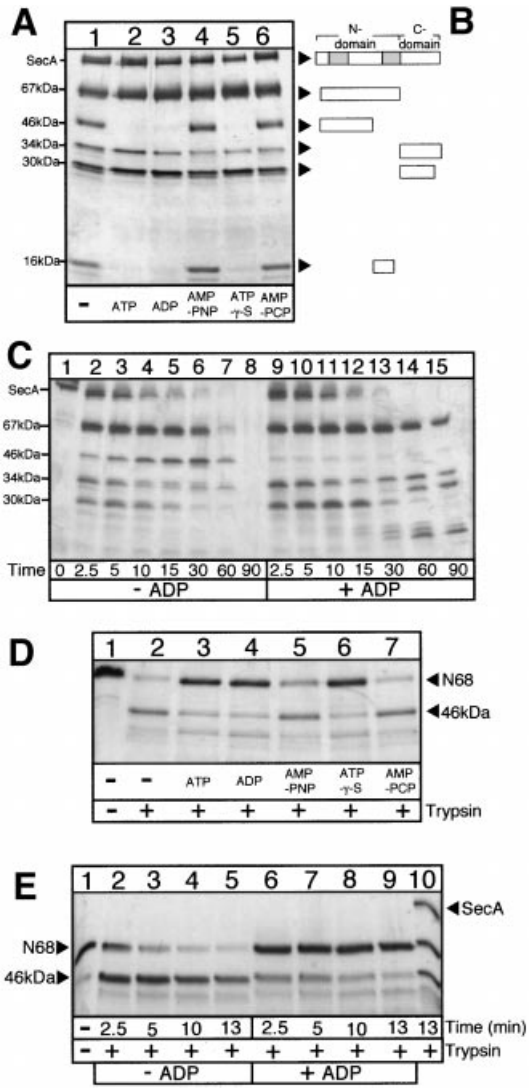

Fig. 2. ADP-stabilized conformations of SecA and the N-domain.
A. Effect of nucleotides on SecA-limited trypsinolysis. SecA (18 μg) was incubated with the indicated nucleotide (1 mM; lanes 2–6) (20 μl, 5 min, on ice, in buffer B). Added trypsin (25 μg ml^{-1}) was inactivated after 13 min (0°C) with Pefabloc (8 mM).
B. SecA tryptic fragments. The N-terminal residues are: for the 67 kDa and 46 kDa fragments, Val–Phe–Gly–Ser–Arg–Asn–Asp–Arg, starting at position 9; for the 34 kDa and 30 kDa fragments, Lys–Leu–Gly–Met–Lys–Pro–Gly–Glu, starting at position 609. For the 20 kDa: Arg–Lys–Asp–Leu–Pro–Asp–Leu–Val, starting at position 420.
C. Effect of ADP on SecA trypsinolysis kinetics. Reactions were the same as in A. At the indicated time points, Pefabloc was added to an aliquot from each sample.
D. Effect of nucleotides on N68 trypsinolysis. N68 (18 μg) reactions were the same as in A.
E. ATP effect on N68 trypsinolysis kinetics. Reactions were the same as in A. Lane 10, SecA trypsinolysis control.

bound to soluble SecA gets immediately hydrolysed. Under these conditions, no extensive ATP hydrolysis occurs (see below) and single ATP turnovers are sufficient for ADP generation. ADP·SecA has a stabilized N-domain because Arg-419 is concealed. Nucleotide binding to the N-domain does not require the C-domain. However, N-domain·ADP stabilizes the C-domain, presumably through their physical interaction.

ADP stabilizes the N-domain by binding at NBD1

We next determined which of the two NBDs is important for the ADP-stabilized conformation of SecA. Mutants D209N-SecA and R509K-SecA (Mitchel and Oliver, 1993) were used. D209N-SecA binds with reduced affinity but does not hydrolyse ATP at NBD1, whereas R509K shows no measurable ATP binding at NBD2. R509K-SecA (Fig. 3A) displays a limited trypsinolysis profile indistinguishable from that of SecA (Fig. 2A), suggesting that NBD2 is not involved in N-domain stabilization. In contrast, D209N-SecA cannot undergo the ADP-driven conformational change and maintains a stable 46 kDa fragment (Fig. 3B, lanes 2 and 3) unless higher ADP levels are used (lane 4). Identical results were obtained with D209N-N68 and R509K-N68 (not shown).

These data demonstrate that ATP has to be hydrolysed at NBD1 in order to induce the ADP conformational state. Binding of ADP *per se* and not the hydrolysis of ATP is responsible for this change. NBD2 does not appear to be involved in this subreaction.

The C-domain is a suppressor of multiple ATP turnovers at NBD1

To examine whether the C-domain is required for multiple rounds of ATP hydrolysis at NBD1, the ATPase activities of N68 and SecA were compared (Fig. 4A). ATP hydrolysis by either enzyme is barely measurable at 0°C (lanes 1 and 5). However, at 37°C, N68 ATPase activity is remarkably elevated (lane 6) when compared with that of SecA (lane 2). The K_m for ATP hydrolysis by N68 (Table 1) is similar to the binding affinity for ADP at NBD1 (0.13 mM; Mitchell and Oliver, 1993), indicating that elevated N68 ATP hydrolysis takes place at NBD1. In agreement with this, the D209N mutation practically eliminates N68 ATPase activity (lane 7). Interestingly, the R509K mutation also reduces ATP hydrolysis at NBD1 but does not abolish it completely (lane 8), suggesting that NBD2 is important for regulation but not catalysis. The R509K mutation has a similar effect on translocation and basal ATPase activity of SecA (lane 4; Mitchel and Oliver, 1993).

As removal of the C-domain unleashes high-level ATP hydrolysis at NBD1, this domain may contain an intramolecular suppressor activity. To test this, N68 supplemented with increasing amounts of C34 was assayed for ATP hydrolysis (Fig. 4B). Concentrations higher than sixfold molar excess of C34 reduce N68 ATPase activity down

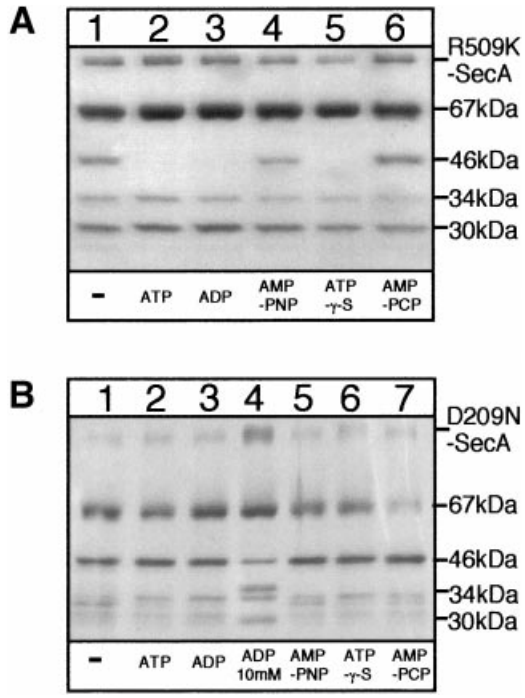

Fig. 3. ADP stabilizes the N-domain by binding at NBD1.
A. NBD2 is not required for ADP stabilization of the N-domain.
B. ADP binding at NBD1 is required for stabilization of the N-domain. R509K-SecA (A) and D209N-SecA (B), preincubated with the indicated nucleotide (1 mM, unless indicated otherwise), were subjected to limited trypsinolysis and were analysed as in Fig. 2A (A 15% and B 12% polyacrylamide).

to SecA levels (Fig. 4B). N68 ATPase suppression by C34 correlates directly with physical assembly of reconstituted SecA dimers and represents functional reconstitution of basal SecA ATPase (Fig. 1D and E).

We conclude that N68 is the minimal SecA domain capable of multiple rounds of ATP hydrolysis. Cytoplasmic SecA basal ATPase is low because of suppression of high-level N-domain ATPase by a C-domain element. We termed this element IRA (intramolecular regulator of ATPase) and determined its identity (described below).

Localization of the IRA element in the SecY-binding region

We hypothesized that, if essential, the IRA region would be conserved. The C-domain contains only two such regions: motif XII, residues 630–678, and motif XIII, residues 767–818 (Sianidis *et al.*, in preparation). We focused on motif XIII (Fig. 4C) because C-terminal truncation derivatives devoid of motif XIII display elevated basal ATPase activity (Breukink *et al.*, 1995; Hirano *et al.*, 1996).

Mutations identified *in vivo* within motif XIII display dominant phenotypes: either strong (*secA::788–789*) or very strong and cold-sensitive *(secAΔ783–795)* (Jarosik and Oliver, 1991). In SecAΔ783–795, 13 aminoacyl residues have been deleted and replaced by five residues, whereas SecA::788–789 has a tripeptide insertion at position 788 (Fig. 4C). The mutant proteins, which are very stable, were purified and characterized by far-UV CD spectroscopy. Spectra for SecA, SecAΔ783–795 and SecA::788–789 are nearly identical, with prominent minima at 208 and 222 nm (Fig. 5A, lower trace) that disappear after denaturation (upper trace). Furthermore, the three proteins have practically superimposable thermal denaturation curves (data not shown) and similar melting temperatures (T_m; 41.1°C, 40.5°C and 39°C respectively). Identical results were obtained with C-domain IRA mutant derivatives (data not shown). We conclude that the IRA mutants have no detectable secondary structure defect.

Both mutants display ADP-driven N-domain stabilization (data not shown), a subreaction that is independent of the C-domain. Interestingly, SecAΔ783–795 exhibits a drastically elevated basal ATPase activity, approaching that of N68 (Fig. 4A, lane 9). SecA::788–789 displays a smaller but highly reproducible increase (≈ 15%; lane 10) over SecA basal ATPase. The K_m for ATP hydrolysis by SecAΔ783–795 or SecA::788–789 (Table 1) is indicative of hydrolysis at NBD1. C34 derivatives carrying the IRA mutations are defective in N68 ATPase suppression (Fig. 4B). Modest (50%) suppression of N68 ATPase is observed only after the addition of high amounts of C34::788–789, whereas C34Δ783–795 is completely defective.

These findings suggest that the IRA function lies within a segment or within the whole of motif XIII (Fig. 4C). Importantly, motif XIII is contained within the SecY-binding and SecA dimerization region (Hirano *et al.*, 1996; Snyders *et al.*, 1997). IRA residues are very polar (Fig. 4C), may be solvent exposed and potentially available for binding interactions with the N-domain and/or another C-domain and/or SecY.

The IRA element is essential for N-/C-domain communication

What is the precise molecular defect of the IRA mutants leading to lack of suppression of N-domain ATPase activity? Because the IRA element is contained within the dimerization region (Fig. 4C; Hirano *et al.*, 1996), one possibility is that its mutation causes defective protomer–protomer assembly. However, DSP [dithiobis (succinimidyl propionate)]-mediated cross-linking (Fig. 5B) reveals dimers and oligomers derived from SecA (lane 5), SecAΔ783–795 (lane 7) and SecA::788–789 (lane 9) with similar yields. Furthermore, the two SecA IRA mutants (Fig. 5C) and their C34 derivatives (Fig. 5D and E) are dimeric, as determined by gel filtration. Therefore, the SecA IRA mutants are not defective in dimerization, but rather in intraprotomer communication between the primary domains. To test this further, we used size exclusion chromatography to examine

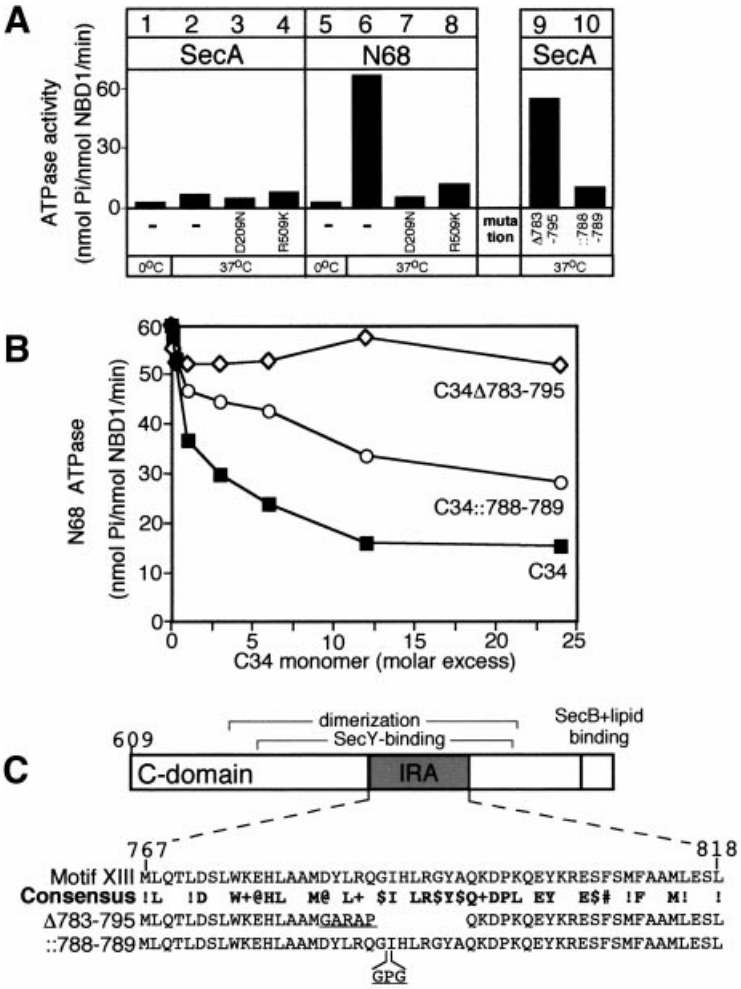

Fig. 4. The C-domain contains an intramolecular regulator of ATP hydrolysis at NBD1.
A. N68 ATP hydrolysis occurs at NBD1. ATPase activity of SecA and derivatives was determined as has been described previously (Lill *et al*., 1990).
B. Suppression of N-domain ATPase by the C-domain requires the IRA element. N68 supplemented with C34 or derivatives was incubated as in Fig. 1D and basal ATPase activity of each reaction was determined (Lill *et al*., 1990). C34 background was subtracted.
C. Motif XIII of SecA. The conserved SecA motif XIII (residues 767–818), within the proposed dimerization and SecY binding domain of SecA, is shown. The consensus (70% identity and/or similarity) was deduced from sequences of 51 SecA homologues. !, Ile, Val, Leu, Met; $, Ala, Gly; #, Phe, Trp, Tyr; @, Asp, Glu; +, Arg, Lys. Residues deleted/added in SecAΔ783–795 or inserted in SecA::788–789 are underlined.

the ability of the C34Δ783–795 and C34::788–789 dimers to interact with the N-domain, leading to formation of reconstituted full-length SecA. N68 mixed with C34::788–789 (molar ratio 1:1) forms a reconstituted species (Fig. 5E) that chromatographs identically to SecA::788–789 (Fig. 5C). In contrast, mixtures of N68 with C34Δ783–795 do not form any reconstituted complexes (Fig. 5D) of the size of full-length SecAΔ783–795 (Fig. 5C). Even at high excess of C34Δ783–795 (not shown), two chromatographically distinct peaks were always observed, indicating lack of physical interaction between N68 and C34Δ783–795.

We conclude that aminoacyl residues within the C-domain IRA element are essential for binding to the N-domain. This binding reaction subsequently regulates ATP hydrolysis at NBD1.

Table 1. Kinetic parameters of ATP hydrolysis. Reactions containing SecA derivatives and ATP (0–2000 μM in buffer B) were incubated (37°C,15 min). Released phosphate was measured as has been described previously (Lill *et al*., 1990).

	Protein			
	SecA	N68	SecAΔ783–795	SecA::788–789
K_m	0.21	0.2	0.23	0.19
V_{max}	5.6	17.2	12	8

K_m is in μM; V_{max} is in nmol Pi per nmol NBD1 per min.

The IRA element is essential for protein translocation and cell viability

To test whether IRA-mediated regulation is essential for translocation, the IRA mutants were examined *in vivo* by genetic complementation (Fig. 6A). Plasmids carrying *secAΔ783–795* and *secA::788–789* were introduced into BL21.19, a thermosensitive *secA* strain (Mitchel and Oliver, 1993). BL21.19 grows at 42°C when it carries a cloned *secA* gene (Fig. 6A, lane 2), but not when carrying the vector alone (Fig. 6A, lane 1). Neither IRA mutant complements BL21.19 (Fig. 6A, lanes 3 and 4), demonstrating that the mutations affect a functionally essential SecA region.

The translocation ability of the IRA mutants was tested *in vitro* using [^{35}S]-proOmpA and reconstituted SecYEG proteoliposomes (Fig. 6B). SecA is very efficient in catalysing ATP-driven [^{35}S]-proOmpA translocation (Fig. 6B, lanes 2 and 3). Pro-OmpA is completely proteolysed only after membrane solubilization with Triton X-100 (Fig. 6B, lane 6). In contrast, neither SecAΔ783–795 (Fig. 6B, lane 4) nor SecA::788–789 (Fig. 6B, lane 5) catalyse any detectable translocation. Similar results were obtained with inverted inner membrane vesicles (IMVs) (not shown).

The extreme C-terminus of SecA binds phospholipids (Breukink *et al*., 1995) and this reaction might be affected in the IRA mutants. We examined this by studying SecA binding and insertion in lipid bilayers, a nucleotide-modulated reaction (Breukink *et al*., 1992; Ulbrandt *et al*., 1992). For the purpose of this experiment, we developed a quantitative, reversible, lipid-binding assay using a resonant mirror biosensor (Fig. 6C; see *Experimental procedures*). SecA binding to immobilized phospholipids is rapid and efficient (Fig. 6C, lane 1) and almost totally inhibited by ATP (Fig. 6C, lane 2) but not by AMP-PNP (Fig. 6C, lane 3) (Breukink *et al*., 1992). Under the same conditions, binding of SecAΔ783–795 (Fig. 6C, lanes 4–6) and SecA::788–789 (Fig. 6C, lanes 7–9) to lipid occurs with final yields and kinetics similar to those of SecA. We conclude that the translocation defect of the IRA mutants is not due to defective lipid binding. Rather, SecAΔ783–795 and SecA::788–789 have a specific SecYEG interaction defect and that intramolecular regulation of ATP hydrolysis is essential for translocation.

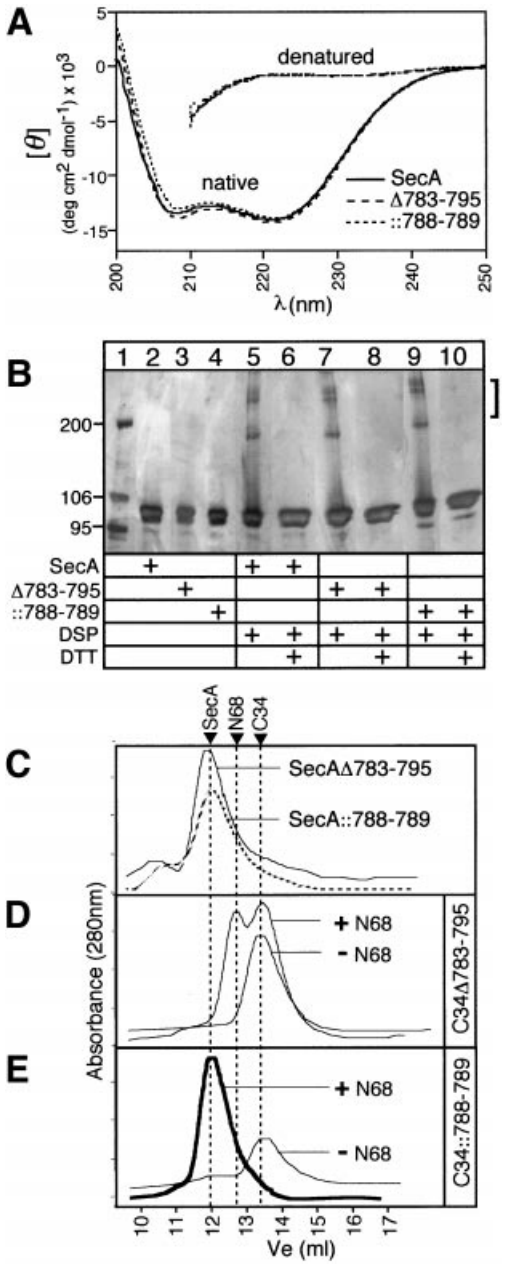

Fig. 5. Structural characterization of SecA mutants.
A. Far-UV CD spectra of SecA and mutant proteins. Experiments were carried out at ambient temperature and samples were normalized for protein concentration. Traces of native and 6 M GnHCl-denatured polypeptides are shown. Increased GnHCl-derived background prevents data collection below 210 nm. θ, mean molar residue ellipticity.
B. SecA dimerization is not affected by IRA mutations. DSP cross-linking of SecA, SecAΔ783–795 and SecA::788–789 was as in Fig. 1B (6% gels). Lane 1, MW standards. Cross-linked species indicated by the bracket.
C–E. Size exclusion chromatography. All samples were chromatographed under identical conditions in the same column, as described in Fig. 1E. Arrows at top of C indicate the migration positions of SecA, N68 and C34.
C. SecAΔ783–795, SecA::788–789 and SecA (120 μg) were analysed in two separate chromatographs and the resulting traces were superimposed in the same graph.
D. C34Δ783–795 (60 μg) alone (labelled '–N68') or mixed with N68 (120 μg) (labelled '+N68') were analysed in two separate experiments and the two resulting chromatograms were superimposed in the same graph.
E. C34::788–789 (60 μg) alone or mixed with N68 as in D. Bold line, reconstituted SecA::788–789.

Interaction of SecA IRA mutants with SecYEG is non-productive

To investigate whether the IRA mutants bind to SecYEG, their ability to compete with SecA was tested. *In vitro* translocation reactions containing [^{35}S]-proOmpA and IMVs were supplemented with SecA or one of the IRA mutants (Fig. 6D). IMVs contain significant amounts of endogenous SecA and are competent for ATP-driven translocation (Fig. 6D, lanes 2 and 3). The addition of excess of SecA increases the yield of translocation (Fig. 6D, lane 4; Yamada *et al*., 1989). Significantly, both SecAΔ783–795 (Fig. 6D, lane 5) and SecA::788–789 (Fig. 6D, lane 6) inhibit protein translocation completely.

This observation clearly shows that the two mutants are proficient in binding to their membrane receptor (SecY) and explains their *in vivo* dominance (Jarosik and Oliver, 1991). Furthermore, it demonstrates that the mutant proteins are competent in displacing endogenous SecA.

Finally, we examined the ATPase activities of the IRA mutants under membrane association conditions (Fig. 6E). SecA displays membrane and translocation ATPase activities (Fig. 6E, lanes 2 and 3; Lill *et al.*, 1990). Neither IRA mutant ATPase activity is stimulated by the addition of IMVs (Fig. 6E, lanes 5 and 8) and/or substrate (Fig. 6E, lanes 6 and 9). In the case of SecAΔ783–795, lack of stimulation of its elevated ATPase activity is not due to saturation of the catalytic capacity of the enzyme. T109N-SecA (Mitchel and Oliver, 1993), which displays a high basal ATPase activity, is further stimulated in the presence of ligands (data not shown). We conclude that although the IRA element mutants bind to SecY they are unable to become activated for subsequent catalysis.

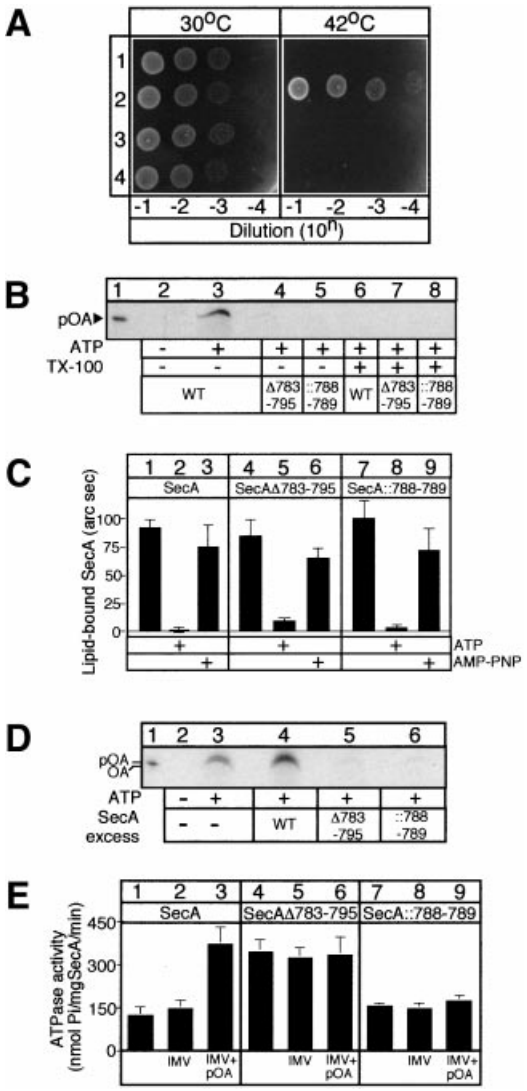

Fig. 6. The IRA element is essential for protein translocation and viability.
A. Genetic complementation. BL21.19 cultures, carrying plasmid derivatives of vector pET5 with cloned *sec*A, *secAΔ783–795* or *secA::788–789* genes as indicated, were adjusted to the same density. Indicated dilutions were spotted on Luria–Bertani (LB)/ampicillin plates.
B. The IRA mutants are defective for preprotein translocation. Reactions (100 μl in buffer B) containing 40 μg ml^{-1} SecA, SecAΔ783–795 or SecA::788–789, [^{35}S]-proOmpA (≈ 50 000 c.p.m.) and SecYEG-proteoliposomes were incubated for 30 min at 37°C. After trypsinolysis (15 min, 1 mg ml^{-1}, 0°C), samples were analysed by SDS–PAGE and fluorography as has been described previously (Economou and Wickner, 1994). Lane 1, 10% of input [^{35}S]-proOmpA (pOA).
C. IRA mutants are not affected in lipid interaction. Binding of SecA and IRA mutants (1 μg; 100 μl buffer B) to lipid was quantified by a resonant mirror biosensor. Nucleotides (2 mM; added as indicated) were preincubated with proteins (25°C; 5 min) before addition to the cuvette. One arc s unit corresponds to 1.6 pg bound protein mm^{-2} of lipid surface.
D. The IRA mutants competitively inhibit preprotein translocation. SecA, SecAΔ783–795 and SecA::788–789 (4 μg) were added to complete *in vitro* translocation reactions (as in B, but containing 200 μg ml^{-1} KM-9 IMVs). Lane 1, 10% of input [^{35}S]-proOmpA.
E. The IRA mutants are defective in membrane and translocation ATPase activity. Basal, membrane (120 μg ml^{-1} urea-treated IMVs) and translocation (IMVs plus 60 μg ml^{-1} proOmpA) ATPase activities of 40 μg ml^{-1} SecA, SecAΔ783–795 or SecA::788–789 were determined (Lill *et al.*, 1990).

Discussion

We have unravelled the molecular mechanism coupling SecA ATP hydrolysis to preprotein translocation. This novel and exciting mechanism derives from the modular nature of SecA architecture, permitting division of labour (Fig. 7). (i) Each protomer comprises two structural elements, the N- and C-domain. (ii) The N-domain contains both NBD1 and NBD2 activities, forming the ATPase core. This region is homologous to DEAD RNA helicases (Koonin and Gorbalenya, 1992; Economou, 1998). N66, which is only 26 residues shorter, is insoluble and has no ATPase activity (Matsuyama *et al.*, 1990; Hirano *et al.*, 1996). (iii) The C-domain mediates dimerization (Fig. 1; Hirano *et al.*, 1996). (iv) N- and C-domains are physically juxtaposed in each protomer, explaining how C-terminal fragments assist folding of N-terminal peptides (Matsuyama *et al.*, 1990). This association allows the enzymatic properties of the two domains to be closely intertwined. (v) N-/C-domain binding requires the IRA element, which encompasses at least part of the conserved motif XIII sequence (Fig. 4C; Fig. 7, arrow a). The phenotypic severity of IRA mutations suggests that the IRA element is the primary contact site between the two domains. Additional C-domain residues may contribute to the bind-

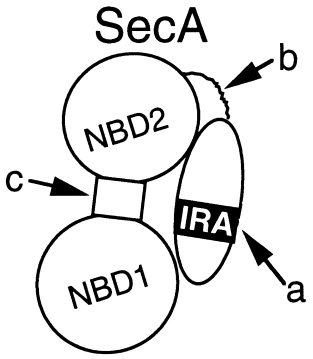

Fig. 7. Domain architecture of the SecA protomer (see text for details).

ing interface. The fact that the ::788–789 mutation does not prevent N-/C-domain binding, but is still functionally compromised, indicates that the IRA element is not a mere interdomain bridge. (vi) The linker connecting the primary domains (Fig. 7, arrow b) is also important. Reconstituted SecA is not translocation competent, although it is dimeric (Fig. 1D and E), it binds to SecY and retains basal ATPase activity (Fig. 4B; E. Vrontou and A. Economou., unpublished). This linker could facilitate SecA intrinsic flexibility during catalysis by allowing 'hinge' or 'shear' domain movements (Argos, 1990; Gerstein *et al*., 1994). (vii) The region of SecA located between the two NBDs and containing Arg-419 (Fig. 7, arrow c) has been implicated in substrate binding (Fikes and Bassford, 1989; Kimura *et al*., 1991). Solvent exposure of this region changes upon SecA binding of ADP (Fig. 2; den Blaauwen *et al*., 1996) or ATP (Ramamurthy and Oliver, 1997). This region may be located at the interdomain interface, as suggested by proteolysis kinetics (Fig. 2), and could facilitate NBD1/NBD2 communication.

Functional isolation of the ATPase core in the absence of the C-domain allowed us to determine the fundamental enzymatic features of SecA ATP hydrolysis. NBD1 rapidly hydrolyses ATP to ADP in a single catalytic round (Fig. 2D and E). This is an inherent temperature-independent property of NBD1 and is abolished by the D209N mutation. However, subsequent multiple ATP turnovers at NBD1 require both a physiological temperature and NBD2 (Fig. 4A). It seems likely that ADP and/or Pi release from NBD1 is a rate-limiting step. Bound ADP makes the N-domain 'tighter' (Fig. 2C and D). This induced fit mechanism could allow NBD2 to exert its effect through physical contacts by bringing it in closer proximity to NBD1. Communication between NBDs is in agreement with double mutant analysis (Mitchel and Oliver, 1993). In DEAD RNA helicases, ATP hydrolysis is regulated by direct physical contact and/or spatial proximity of catalytic and regulatory residues (Yao *et al*., 1997; Cho *et al*., 1998; Kim *et al*., 1998; Velankar *et al*., 1999). Our data decipher the as yet elusive role of NBD2 as a regulatory site optimizing ATP turnover rates at NBD1.

Functional reconstitution of basal SecA ATPase revealed that the N-domain ATPase is regulated by the C-domain (Fig. 4A and B). In cytoplasmic SecA, binding of the IRA sequence to the N-domain stabilizes the ADP state and prevents multiple ATP turnovers at NBD1 (Fig. 4B). When the IRA switch is disabled (Fig. 4A; Breukink *et al*., 1995; Hirano *et al*., 1996; Price *et al*., 1996), the N-domain ATPase becomes unregulated. ADP-mediated stabilization of the N-domain (see above) is transmitted to the C-domain (Fig. 2), a flexible domain displaying molten globule characteristics (Song and Kim, 1997). This results in a 'closed' more compact SecA structure (Fig. 2; den Blaauwen *et al*., 1996) distinct from the 'open' structure of the apoprotein and of the ATP-bound state (Fig. 2; den Blaauwen *et al*., 1996; Song and Kim, 1997). Considering cellular ATP concentrations and the high affinity of NBD1 for ADP (Mitchel and Oliver, 1993), most of the cytoplasmic SecA is likely to exist in the ADP state. IRA suppression of SecA ATPase and stabilization of the 'closed' state have three major consequences: (i) as SecA·ADP is prevented from non-specific associations with lipid (Fig. 6C; Breukink *et al*., 1992), productive interactions with SecYEG are favoured; (ii) accessibility of substrate to the N-domain (Fikes and Bassford, 1989; Kimura *et al*., 1991) and of SecB to the extreme C-terminus (Breukink *et al*., 1995; den Blaauwen *et al*., 1997; Fekkes *et al*., 1997, 1998) is prevented; and (iii) vain ATP hydrolysis in the cytoplasm is avoided.

Remarkably, the C-domain is also responsible for delivering the soluble ATP chemistry to the membrane by specifically recognizing SecY (Economou and Wickner, 1994; Matsumoto *et al*., 1997; Ramamurthy and Oliver, 1997; Snyders *et al*., 1997). This targeting mechanism is reminiscent of two-component bacterial toxins such as diphtheria, in which a membrane translocator/receptor binding domain (B chain) facilitates the transmembrane crossing of the catalytic domain (A chain; Ren *et al*., 1999). The IRA mutations we tested do not prevent SecY binding (Fig. 6D) and therefore the affected residues, although proximal (Fig. 4C), are not part of the binding site proper. Binding of the C-domain to SecY leads to partial stimulation of ATP hydrolysis (membrane ATPase; Lill *et al*., 1990) and increases dramatically SecA affinity for substrate (Hartl *et al*., 1990) and SecB (den Blaauwen *et al*., 1997; Fekkes *et al*., 1997, 1998). In a reaction that may mimic the SecY-induced effect, limited unfolding of the C-domain by chaotropes increases basal ATPase activity (Song and Kim, 1997). Similarly, binding to model membranes causes localized SecA unfolding (Breukink *et al*., 1992, 1995; Ulbrandt *et al*., 1992; Song and Kim, 1997) attributed largely to the C-domain (Song and Kim, 1997) and stimulates substrate binding and

lipid ATPase activity (Lill *et al*., 1990). These data suggest that SecY 'primes' SecA for translocation by causing C-domain conformational changes that are 'sensed' by IRA and partially relieve IRA-mediated ATPase suppression. The location of IRA within the SecY binding region is expected to allow direct sensing of SecY interactions. IRA-mediated ATPase suppression is completely switched off only after formation of the translocase/substrate ternary complex.

Our data indicate a molecular mechanism for coupling of ATP hydrolysis to preprotein translocation mediated by the IRA switch: substrates trigger SecA membrane cycling by binding to the N-domain (Fikes and Bassford, 1989; Kimura *et al*., 1991) and causing ADP release (Shinkai *et al*., 1991), thus converting SecA to the 'open' state. It is not known whether substrates may also associate with the C-domain, thus masking IRA-mediated stabilization of the ADP state. Because the flexible C-domain is no longer restrained by N-domain interactions, fresh ATP binding can drive its membrane insertion (Economou and Wickner, 1994). C-domain membrane penetration may co-transfer the attached N-domain (Eichler and Wickner, 1997; Ramamurthy and Oliver, 1997) together with bound substrate (Schiebel *et al*., 1991; van der Wolk *et al*., 1997) deeper into the membrane plane. A single round of ATP hydrolysis reverts SecA to the 'closed' ADP state. The N-domain 'tightens', releases the substrate (Schiebel *et al*., 1991) and rebinds to the IRA switch. ADP is sufficient to drive deinsertion because D209N-SecA, which is unable to acquire the ADP conformation (Fig. 3B), can insert in the membrane but cannot deinsert (Economou *et al*., 1995). Each cycle of ATP binding and hydrolysis is therefore tightly coupled to a SecA membrane insertion/deinsertion stroke, which is coupled to translocation of a defined preprotein segment. Coupling is mediated by the IRA switch through localized conformational changes 'sensed' by Trp-775 (Fig. 4C; den Blaauwen *et al*., 1996), leading to precise binding and release reactions with the N-domain. Deletion of the IRA switch uncouples multiple rounds of N-domain ATP hydrolysis from ongoing translocation (Fig. 4A). Although a single round of ATP hydrolysis is sufficient for conversion of 'open' inserted SecA to the 'closed' ADP-bound deinsertion state (Fig. 2), for translocation of complete preprotein chains multiple rounds of ATP hydrolysis must occur (Lill *et al*., 1990; Schiebel *et al*., 1991; van der Wolk *et al*., 1997), driving multiple rounds of SecA cycling (Economou and Wickner, 1994; Economou *et al*., 1995). This explains why NBD2, which is essential for multiple (Fig. 4A; Mitchel and Oliver, 1993) but not for single (Fig. 3A) ATP turnovers at NBD1, is not required for SecA deinsertion (Economou *et al*., 1995), but is essential for complete protein translocation (Mitchel and Oliver, 1993; Economou *et al*., 1995). An obvious as well as exciting mechanistic possibility is that the IRA switch regulates ATP turnovers at NBD1 *in trans* through direct interaction with the *cis* regulatory element NBD2.

Dissection of the complex SecA molecule in functional domains amenable to biochemical analysis provides us with novel and powerful tools to quantify precisely the molecular interactions and structure of translocase domains. We are now in a position to determine in molecular detail the role of each SecA protomer and their conformational dynamics regulated by substrate and nucleotides.

Experimental procedures

Bacterial strains and recombinant DNA experiments

Escherichia coli strains DH5α, JM109, BL21(λDE3) and BL21.19 (Mitchel and Oliver, 1993) carrying various plasmids were used. Growth and manipulations were as has been described previously (Economou and Wickner, 1994). DNA manipulations were as described by Ausubel *et al*. (1994). The identity of all constructs was confirmed using DNA sequencing and/or restriction analysis.

IRA mutant overexpression. pIMBB2 (SecAΔ783–795) and pIMBB4 (SecA::788–789) were generated upon replacement of the 2.5 kb *Nco*I fragment of pIMBB10 (a pZ52-SecA derivative; Schmidt *et al*., 1988) with the corresponding one from pGJ3 or pGJ10 (Jarosik and Oliver, 1991).

secA mutagenesis. The 4.8 kb *Bam*HI fragment from pZ52-SecA, containing the *secA* coding sequence, was cloned in the *Bam*HI site of pALTER-EX1 (Promega) to generate pIMBB23. Mutagenized *secA* derivatives (ALTERED-SITES II protocol; Promega) were subcloned into pIMBB10.

N68 overexpression. Using oligonucleotide X12 (GCATGA TGCGTAAATAGGGTATGAAGCC), an amber stop codon was introduced in *secA*, on pIMBB23, giving rise to pIMBB16. The 2.5 kb *Nco*I fragment of pIMBB10 was replaced by the corresponding one from pIMBB16, resulting in pIMBB8.

C34 overexpression. Using oligonucleotides X10 (GAGATT TTATTATGCATATCAAATTGTTAAC) and X11 (GGCATG ATGCATAAACTGGG), two *Nsi*I sites were introduced in *secA*, on pIMBB23, generating pIMBB18. Both mutations (in methionine codons 1 and 607) are silent. pIMBB17 was derived from pIMBB18, after *Nsi*I fragment removal and religation. pIMBB5 was generated when the 1.1 kb *Eco*RI (made blunt)– *Nco*I fragment from pIMBB17 was cloned in the *Nco*I site of pIMBB10, after *Bam*HI (made blunt)– NcoI digestion.

Hexahistidine tagging. To construct N-terminal His-N68, pIMBB7 encoding His-SecA (Sianidis *et al*. in preparation) was used. The 2.3 kb *Nco*I fragment from pIMBB8 replaced the *Nco*I fragment of pIMBB7 to form pIMBB28. To construct His-D209N-N68 (pIMBB32) and His-R509K-N68 (pIMBB69), the 1.9 kb *Bam*HI–*Kpn*I fragment of either mutant gene (Mitchel and Oliver, 1993) replaced the corresponding

fragment on pIMBB28. To construct His-C34, pIMBB5 was digested with *Nsi*I and ligated in the presence of X34 (TCATCATCATCATCATCATATGCA) and X35 (TATGA TGATGATGATGATGATGCA) and resulted in pIMBB70. His-C34Δ783–795 (pIMBB71) and His-C34::788–789 (pIMBB72) were constructed by replacing the 0.8 kb, *Eco*RI–*Mfe*I fragment of pIMBB70 with the corresponding one from either pIMBB2 or pIMBB4.

GST-C34. To fuse the C34 sequence in frame to the C-terminus of the glutathione-S-transferase from *Schistosoma japonicum,* the 1.17 kb *Eco*RI–*Nsi*I fragment from pIMBB5 was cloned into *Eco*RI–*Pst*I-digested pBSIIKS (Stratagene) to form pIMBB35. An *Eco*RI–*Bam*HI fragment from pIMBB35 was inserted in the corresponding sites of pGEX-2T (Pharmacia) to generate pIMBB36.

Chemicals and biochemicals

Proteinase K, TPCK-treated trypsin, the trypsin inhibitor Pefabloc [4-(2-aminoethyl)-benzenesulphonyl fluoride], phenylmethylsulphonyl fluoride (PMSF), AMP-PNP (adenylyl-imidodiphosphate), adenylyl-(β,γ-methylene)-diphosphonate (AMP-PCP), ATP, ADP and ATP-γ-S [adenosine-5′-o-(3-thiotriphosphate)] were from Boehringer Mannheim. Dithiothreitol (DTT), SDS, lysozyme, nucleases, Coomassie brilliant blue, detergents, imidazole and lipid-free bovine serum albumin (BSA) were from Sigma. Restriction enzymes, T4 ligase and calf alkaline phosphatase were from Minotech; oligonucleotides from the IMBB Microchemistry Facility. dNTPs were from Promega. Sequenase and [^{35}S]-labelled dNTPs were from Amersham. The homobifunctional cross-linker DSP (dithiobis [succinimidyl propionate]) was from Pierce.

Protein purification and chromatography

SecA and derivatives were purified as has been described previously (Lill *et al*., 1990; Mitchel and Oliver, 1993), using Pharmacia resins. His-tagged polypeptides were purified on nickel-nitrilotriacetic acid agarose (Qiagen), according to the manufacturer's instructions. Purified proteins were stored at −80°C.

N68 purification. Cytosolic polypeptides from BL21.19/pIMBB8 cells were precipitated by $(NH_4)_2SO_4$ (50% saturation) and collected by centrifugation (Sorvall, JA20 rotor, 4°C, 20 min, 10 000 r.p.m.). The pellet was redissolved in buffer PS (50 mM tris-HCl, pH 8, 1 M $(NH_4)_2SO_4$, 1 mM DTT) and loaded onto a PhenylSepharose Fast Flow resin (equilibrated with buffer PS). After extensive washes (PS buffer), a 1–0 M $(NH_4)_2SO_4$ linear gradient was applied and fractions were collected. The N68 peak fractions were pooled and loaded onto a Fast Flow Q Sepharose resin (equilibrated in 50 mM tris-HCl, pH 8). N68 was eluted in a 0–1 M NaCl linear gradient.

Size exclusion chromatography. A prepacked Superdex 200HR 10/30 fast protein liquid chromatography (FPLC) column (10–600 kDa separation range), equilibrated with 50 mM Tris-HCl, pH 8, 300 mM NaCl, 5 mM β-mercaptoethanol buffer, was used at 4°C at a flow rate 0.5 ml min^{-1}. Samples were injected via a V-7 valve, using a 200 μl loop. MW markers were from Boehringer Mannheim. Blue Dextran 2000 was from Pharmacia. MW determination was as recommended (Pharmacia).

GST-C34 and His-N68 immobilization

GST or GST-C34 from cytosolic extracts were immobilized on glutathione sepharose and His-N68 was immobilized on Ni^{2+}-NTA agarose, as described by the manufacturers. Briefly, 100 μl resin suspension was centrifuged (3 min; 3000 × *g*) and washed with buffer S (100 mM NaCl, 20 mM Tris-HCl, pH 8, 0.3% NP40, 0.125% BSA). The beads were resuspended in 100 μl buffer S and incubated (30 min, room temperature, gentle rocking) with 500 μg GST-C34 or 250 μg His-N68. NaCl, NP40 and BSA were added in the above mix to 100 mM, 0.3% and 0.125% respectively. Beads were centrifuged as before and washed three times with buffer S.

Circular dichroism thermal stability

Circular dichroism (CD) spectra in the far-ultraviolet range were recorded on a Jasco J-715 spectropolarimeter interfaced with a Peltier element for temperature control. The instrument was calibrated with a 0.10% aqueous solution of d-10-camphor-sulphonic acid. Protein stock solutions (5–7 μM) were in 20 mM MOPS buffer, pH 7.5. Quartz 1 mm path-length cells were used (Hellma). Spectra were recorded at 18°C, with 0.2 nm resolution and were baseline-corrected by subtraction of the buffer spectrum at the same temperature. The combined absorbance of cell, sample and solvent was kept at less than one over the measured range. Thermal denaturation curves were obtained by monitoring the ellipticity at 222 nm while heating the protein samples at 50°C/1 h in covered cuvettes (at least two scans per protein). Curves were analysed, based on a two-state approximation (Becktel and Schellman, 1987) and were fitted using non-linear regression (KALEIDAGRAPH; Abelbeck Software).

Resonant mirror assay

Resonant mirror spectroscopy was carried out using the iAsys system (Affinity Sensors) at 25°C (settings: 75% stirring; 0.8 s data collection). Cuvettes (non-derivatized) were coated with lipids in the presence of 1.25% β-octylglucoside in phosphate buffered saline, pH 7.4 (OG/PBS). The buffer was removed and 50 μl DMPE (2 mg ml^{-1} in 1.25% OG/PBS) was added to the cuvette. After saturation of lipid binding, PBS (3 × 50 μl) was directly added after binding was equilibrated. Binding was monitored for 2 min and the cuvette was regenerated (5 M urea, 2 min, then washed with buffer B). Binding was calculated from the response (arc s) of the first 100 s.

Miscellaneous techniques

Protein concentration was determined using the Bradford reagent (Bio-Rad) with BSA as a standard, by UV absorbance or by amino acid analysis. SecYEG proteoliposomes, SDS–PAGE and fluorography were performed as has been

described previously by Economou *et al.* (1995). Native PAGE was carried out using a Bio-Rad Mini Protean II system. ^{35}S-labelled proteins were synthesized from plasmids pIMBB5 (C34), pIMBB8 (N68) and pTYE009 (proOmpA; Yoshihisa and Ito, 1996) by *in vitro* transcription and translation (Promega), according to the manufacturer's instructions. [^{35}S]-methionine (1000 Ci mmol^{-1}) was from Amersham. Enzymatic parameters were calculated using Enzpack (BioSoft).

Acknowledgements

We are grateful to G. Thireos and K. Tokatlidis for critical comments on the manuscript; B. Pozidis (Minotech) and B. Shilton for help with chromatography; K. Ashman (EMBL) for N-terminal sequencing; M. Weldon and L. Packman (Cambridge University) for amino acid analysis; C. Stassinopoulou and M. Pelekanou (Demokritos NRC) for use of CD facilities; N. Kyrpides for biocomputing; Y. Papanikolau for useful discussions; T. deBoer for plasmid constructs; D. Dialektakis (Minotech) for fermentation; and D. Oliver, K. Ito, D. Tzamarias and H. Tokuda for plasmids. Our research is supported by grants (to A.E.) from the European Union Directorate of Science and Technology (TMR-ERBFMRXCT960035, Biotech2-BIO4-CT97–2244 and Biotech2-BIO4-CT98–0051); the DLR and the Greek Secretariat of Research and Technology (GRI-088-97 to A.E. and A.K; EPETII 97 EKBAN 2-17); and the University of Crete Research Fund (KA 1194).

References

Argos, P. (1990) An investigation of oligopeptides linking domains in protein tertiary structures and possible candidates for general gene fusion. *J Mol Biol* **211:** 943–958.

Ausubel, F.M., Brent, R., Kingston, R.E., Moore, D.D., Smith, J.A., Seidman, J.G., and Struhl, K. (1994) *Current Protocols in Molecular Biology.* New York: John Wiley and Sons.

Becktel, W.J., and Schellman, J.A. (1987) Protein stability curves. *Biopolymers* **26:** 1859–1877.

den Blaauwen, T., Fekkes, P., de Wit, J.G., Kuiper, W., and Driessen, A.J.M. (1996) Domain interactions of the peripheral preprotein translocase subunit SecA. *Biochemistry* **35:** 11194–12004.

den Blaauwen, T., Terpetschnig, E., Lakowicz, J.R., and Driessen, A.J. (1997) Interaction of SecB with soluble SecA. *FEBS Lett* **416:** 35–38.

Breukink, E., Demel, R.A., de Korte-Kool, G., and de Kruijff, B. (1992) SecA insertion into phospholipids is stimulated by negatively charged lipid and inhibited by ATP: a monolayer study. *Biochemistry* **31:** 1119–1124.

Breukink, E., Nouwen, N., van Raalte, A., Mizushima, S., Tommassen, J., and de Kruijff, B. (1995) The C terminus of SecA is involved in both lipid binding and SecB binding. *J Biol Chem* **270:** 7902–7907.

Cho, H.S., Ha, N.C., Kang, L.W., Chung, K.M., Back, S.H., Jang, S.K., and Oh, B.H. (1998) Crystal structure of RNA helicase from genotype 1b hepatitis C virus. A feasible mechanism of unwinding duplex RNA. *J Biol Chem* **273:** 15045–15052.

Danese, P.N., and Silhavy, T.J. (1998) Targeting and assembly of periplasmic and outer-membrane proteins in *Escherichia coli. Annu Rev Genet* **32:** 59–94.

Duong, F., and Wickner, W. (1997a) Distinct catalytic roles of the SecYE, SecG and SecDFyajC subunits of preprotein translocase holoenzyme. *EMBO J* **16:** 2756–2768.

Duong, F., and Wickner, W. (1997b) The SecDFyajC domain of preprotein translocase controls preprotein movement by regulating SecA membrane cycling. *EMBO J* **16:** 4871–4879.

Duong, F., Eichler, J., Price, A., Leonard, M.R., and Wickner, W. (1997) Biogenesis of the Gram-negative bacterial envelope. *Cell* **91:** 567–573.

Economou, A. (1998) Bacterial preprotein translocase, mechanism and conformational dynamics of a processive enzyme. *Mol Microbiol* **27:** 511–518.

Economou, A. (1999) Following the leader: bacterial protein export through the Sec translocase. *Trends Microbiol* **7:** 315–319.

Economou, A., and Wickner, W. (1994) SecA promotes preprotein translocation by undergoing ATP-driven cycles of membrane insertion and deinsertion. *Cell* **78:** 835–843.

Economou, A., Pogliano, J.P., Beckwith, J., Oliver, D.B., and Wickner, W. (1995) SecA membrane cycling at SecYEG is driven by distinct ATP binding and hydrolysis events and is regulated by SecD and SecF. *Cell* **83:** 1171–1181.

Eichler, J., and Wickner, W. (1997) Both an N-terminal 67 kDa domain and a C-terminal 30 kDa domain of SecA cycle into the membrane at SecYEG during translocation. *Proc Natl Acad Sci USA* **94:** 5574–5581.

Fekkes, P., van der Does, C., and Driessen, A.J.M. (1997) The molecular chaperone SecB is released from the carboxy-terminus of SecA during initiation of precursor protein translocation. *EMBO J* **16:** 6095–6113.

Fekkes, P., de Wit, J.G., van der Wolk, J.P., Kimsey, H.H., Kumamoto, C.A., and Driessen, A.J. (1998) Preprotein transfer to the *Escherichia coli* translocase requires the co-operative binding of SecB and the signal sequence to SecA. *Mol Microbiol* **29:** 1179–1190.

Fikes, J.D., and Bassford Jr, P.J. (1989) Novel *secA* alleles improve export of maltose-binding protein synthesized with a defective signal peptide. *J Bacteriol* **171:** 402–409.

Gerstein, M., Lesk, A.M., and Chothia, C. (1994) Structural mechanisms for domain movements in proteins. *Biochemistry* **33:** 6739–6749.

Hartl, F.-U., Lecker, S., Schiebel, E., Hendrick, J.P., and Wickner, W. (1990) The binding of SecB to SecA to SecY/E mediates preprotein targeting to the *E. coli* membrane. *Cell* **63:** 269–279.

Hirano, M., Matsuyama, S., and Tokuda, H. (1996) The carboxyl-terminal region is essential for SecA dimerization. *Biochem Biophys Res Commun* **229:** 90–95.

Jarosik, G.P., and Oliver, D.B. (1991) Isolation and analysis of dominant *secA* mutations in *Escherichia coli. J Bacteriol* **173:** 860–868.

Joly, J.C., and Wickner, W. (1993) The SecA and SecY subunits of translocase are the nearest neighbors of the translocating preprotein, shielding it from phospholipids. *EMBO J* **12:** 255–263.

Kim, Y.J., Rajapandi, T., and Oliver, D.B. (1994) SecA protein is exposed to the periplasmic surface of the *E. coli* inner membrane in its active state. *Cell* **78:** 845–853.

Kim, J.L., Morgenstern, K.A., Griffith, J.P., Dwyer, M.D., Thomson, J.A., Murcko, M.A., *et al.* (1998) Hepatitis C virus NS3 RNA helicase domain with a bound oligonucleotide: the crystal structure provides insights into the mode of unwinding. *Structure* **6:** 89–100.

Kimura, E., Akita, M., Matsuyama, S.-i., and Mizushima, S. (1991) Determination of a region in SecA that interacts with presecretory proteins in *Escherichia coli*. *J Biol Chem* **206:** 6600–6606.

Koonin, E.V., and Gorbalenya, A.E. (1992) Autogenous translation regulation by *Escherichia coli* ATPase SecA may be mediated by an intrinsic RNA helicase activity of this protein. *FEBS Lett* **298:** 6–8.

Lill, R., Dowhan, W., and Wickner, W. (1990) The ATPase activity of SecA is regulated by acidic phospholipids, SecY, and the leader and mature domains of precursor proteins. *Cell* **60:** 271–280.

Matsumoto, G., Yoshihisa, T., and Ito, K. (1997) SecY and SecA interact to allow SecA insertion and protein translocation across the *Escherichia coli* plasma membrane. *EMBO J* **16:** 6384–6393.

Matsuyama, S.-i., Kimura, E., and Mizushima, S. (1990) Complementation of two overlapping fragments of SecA, a protein translocation ATPase of *Escherichia coli,* allows ATP binding to its amino-terminal region. *J Biol Chem* **267:** 8760–8767.

Meyer, T.H., Menetret, J.F., Breitling, R., Miller, K.R., Akey, C.W., and Rapoport, T.A. (1999) The bacterial SecY/E translocation complex forms channel-like structures similar to those of the eukaryotic Sec61p complex. *J Mol Biol* **285:** 1789–1800.

Miller, A., Wang, L., and Kendall, D.A. (1998) Synthetic signal peptides specifically recognize SecA and stimulate ATPase activity in the absence of preprotein. *J Biol Chem* **273:** 11409–11412.

Mitchell, C., and Oliver, D. (1993) Two distinct ATP-binding domains are needed to promote protein export by *Escherichia coli* SecA ATPase. *Mol Microbiol* **10:** 483–497.

Nishiyama, K., Suzuki, T., and Tokuda, H. (1996) Inversion of the membrane topology of SecG coupled with SecA-dependent preprotein translocation. *Cell* **85:** 71–81.

Nishiyama, K., Fukuda, A., Morita, K., and Tokuda, H. (1999) Membrane deinsertion of SecA underlying proton motive force-dependent stimulation of protein translocation. *EMBO J* **18:** 1049–1058.

Park, S.K., Kim, D.W., Choe, J., and Kim, H. (1997) RNA helicase activity of *Escherichia coli* SecA protein. *Biochem Biophys Res Commun* **235:** 593–597.

Price, A., Economou, A., Duong, F., and Wickner, W. (1996) Separable ATPase and membrane insertion domains of the SecA subunit of preprotein translocase. *J Biol Chem* **271:** 31580–31584.

Ramamurthy, V., and Oliver, D.B. (1997) Topology of the integral membrane form of *Escherichia coli* SecA protein reveals multiple periplasmically exposed regions and modulation by ATP binding. *J Biol Chem* **272:** 23239–23246.

Ren, J., Kachel, K., Kim, H., Malenbaum, S.E., Collier, R.J., and London, E. (1999) Interaction of diphtheria toxin T domain with molten globule-like proteins and its implications for translocation. *Science* **284:** 955–957.

Schiebel, E., Driessen, A.J.M., Hartl, F.-U., and Wickner, W. (1991) $\Delta\mu_H^+$ and ATP function at different steps of the catalytic cycle of preprotein translocase. *Cell* **64:** 927–939.

Schmidt, M.G., Rollo, E.E., Grodberg, J., and Oliver, D.B. (1988) Nucleotide sequence of the secA gene and secA (Ts) mutations preventing protein export in *Escherichia coli*. *J Bacteriol* **170:** 3404–3414.

Shilton, B., Svergun, D.I., Volkov, V.V., Koch, M.H.J., Cusack, S., and Economou, A. (1998) *Escherichia coli* SecA shape and dimensions. *FEBS Lett* **436:** 277–282.

Shinkai, A., Mei, L.H., Tokuda, H., and Mizushima, S. (1991) The conformation of SecA, as revealed by its protease sensitivity, is altered upon interaction with ATP, resecretory proteins, everted membrane vesicles, and phospholipids. *J Biol Chem* **266:** 5827–5833.

Snyders, S., Ramamurthy, V., and Oliver, D. (1997) Identification of a region of interaction between *Escherichia coli* SecA and SecY proteins. *J Biol Chem* **272:** 11302–11306.

Song, M., and Kim, H. (1997) Stability and solvent accessibility of SecA protein of *Escherichia coli*. *J Biochem* **122:** 1010–1018.

Tzamarias, D., and Struhl, K. (1994) Functional dissection of the Cyc8–Tup1 transcriptional co-repressor complex in yeast. *Nature* **369:** 758–761.

Uchida, K., Mori, H., and Mizushima, S. (1995) Stepwise movement of preproteins in the process of translocation across the cytoplasmic membrane of *Escherichia coli*. *J Biol Chem* **270:** 30862–30868.

Ulbrandt, N.D., London, E., and Oliver, D.B. (1992) Deep penetration of a portion of *Escherichia coli* SecA protein into model membranes is promoted by anionic phospholipids and by partial unfolding. *J Biol Chem* **267:** 15184–15192.

Velankar, S.S., Soultanas, P., Dillingham, M.S., Subramanya, H.S., and Wigley D.B. (1999) Crystal structures of complexes of PcrA DNA helicase with a DNA substrate indicate an inchworm mechanism. *Cell* **97:** 75–84.

van der Wolk, J.P., de Wit, J.G., and Driessen, A.J. (1997) The catalytic cycle of the *Escherichia coli* SecA ATPase comprises two distinct preprotein translocation events. *EMBO J* **16:** 7297–7304.

Yamada, H., Matsuyama, S.-I., Tokuda, H., and Mizushima, S. (1989) A high concentration of SecA allows proton motive force-independent translocation of a model secretory protein into *Escherichia coli* membrane vesicles. *J Biol Chem* **264:** 18577–18581.

Yao, N., Hesson, T., Cable, M., Hong, Z., Kwong, A.D., Le, H.V., and Weber, P.C. (1997) Structure of the hepatitis C virus RNA helicase domain. *Nature Struct Biol* **4:** 463–467.

Yoshihisa, T., and Ito, K. (1996) Pro-OmpA derivatives with a His_6 tag in their N-terminal 'translocation initiation domains' are arrested by Ni^{2+} at an early post-targeting stage of translocation. *J Biol Chem* **271:** 9429–9436.